Catal Lett (2012) 142:608–614
DOI 10.1007/s10562-012-0805-5

Novel MgO–SnO_2 Solid Superbase as a High-Efficiency Catalyst for One-Pot Solvent-Free Synthesis of Polyfunctionalized 4*H*-pyran Derivatives

Shu-Guo Zhang · Shuang-Feng Yin · Yu-Dan Wei · Sheng-Lian Luo · Chak-Tong Au

Received: 19 January 2012 / Accepted: 10 March 2012 / Published online: 27 March 2012

Abstract We report for the first time the hydrothermal synthesis of MgO–SnO_2 solid superbase using P123 as template. The basicity of the materials was determined by two approaches of Hammett indicators method and temperature-programmed desorption using CO_2 as adsorbate (CO_2-TPD). It was found that Mg/Sn molar ratio has an effect on MgO–SnO_2 basicity, and superbasicity was observed only at Mg/Sn molar ratio of 1. With variation of Mg/Sn molar ratio, superbase strength (H_-) was in the 26.5–33.0 range, showing superbasic value up to 0.939 mmol/g. The structure and texture of the as-prepared materials were studied by powder X-ray diffraction (XRD), scanning electron microscopy (SEM), and N_2 physio-adsorption methods. We detected particles of spherical morphology having diameter of ca. 150 nm. N_2 adsorption–desorption results suggested that the materials are of mesoporous structure, having specific surface area of 115.2 m^2/g and average pore diameter of 6 nm. The superbase was found to exhibit excellent catalytic activity towards the *one-pot* synthesis of polyfunctionalized 4*H*-pyrans through the condensation of aldehydes, malononitrile, and an active methylene compound. Its excellent catalytic efficiency is related to its superbasicity of the MgO–SnO_2. The results provide a new route for the design and preparation of composite oxide superbases. Furthermore, the solid superbases will facilitate a strategy for high-efficiency synthesis of polyfunctionalized 4*H*-pyrans.

S.-G. Zhang · S.-F. Yin (✉) · Y.-D. Wei · S.-L. Luo · C.-T. Au
College of Chemistry and Chemical Engineering, Hunan University, Changsha 410082, Hunan, China
e-mail: sf_yin@hnu.edu.cn

C.-T. Au
Department of Chemistry, Hong Kong Baptist University, Kowloon Tong, Hong Kong

Keywords Solid superbase · MgO–SnO_2 · Condensation reaction · 4*H*-pyrans · Catalyst

1 Introduction

Solid superbases are materials possessing basic sites with strength (H_-) higher than 26 [1]. In the development of environment-benign processes, they are used as catalysts so that reactions can be conducted under mild conditions and without generation of much waste [1–3]. In the past two decades, there were many reports on solid superbases such as NaN_3/γ-Al_2O_3 [4], Na/NaOH/γ-Al_2O_3 [5], K/MgO [6], Eu_2O_3/γ-Al_2O_3 [7], KNO_3/γ-Al_2O_3 [8], KNO_3/ZrO_2 [9], KOH/ZrO_2 [10], KF/γ-Al_2O_3 [11], and $Ca(NO_3)_2$/SBA-15 [12]. Recently, we found that the solid superbases Na_2SnO_3 [13, 14] and KOH/La_2O_3–MgO [15] showed excellent catalytic efficiency towards some organic reactions at room temperature (RT). However, industrial application of solid superbases is limited because most of them are sensitive to O_2 and/or CO_2, hence are difficult to prepare [1, 2]. In addition, conventional solid superbases have low surface area and superbasic sites. It is, therefore, highly desirable to develop high-surface-area solid superbases with more superbasic sites as well as simple preparation and easy storage.

After a systematic survey, we found that the presence of an alkali metal component is rather common among the reported solid superbases [1–3], and reports on composite oxide superbases free of alkali metal component are few. It was regarded that crystal defects and/or vacant sites are needed for the formation of superbasic sites over some superbases [9, 16, 17]. Knowing that SnO_2 is rich in crystal defects [18, 19] and special MgO shows superbasicity [1],

we synthesized MgO–SnO_2 composite superbases, and investigated their potentials in catalytic application.

The synthesis of polyfunctionlized 4*H*-pyrans group has attracted much attention since it is a constituent of various natural products [20–30]. The 4H-pyran derivatives can be used as anti-coagulants, anticancer agents, anti-anaphylactics, photoactive materials, etc. [21, 22]. Many catalysts have been employed to synthesize the 4H-pyran unit, e.g., amino-functionalized ionic liquid [23], tetrabutylammonium bromide [25], tetra-methyl ammonium hydroxide [26], [BMIm]BF_4 [27], SiO_2 [28], piperidine [29], and Mg/La oxide [30]. All of these catalysts have merits, while some have disadvantages or limitations such as harsh reaction conditions, low yields, poor selectivity, tedious work-ups, use of organic solvent, and/or poor recyclability. Thus, the development of a suitable solid catalyst for efficient synthesis of 4H-pyrans in a single step is attractive. We describe herein the synthesis of a novel MgO–SnO_2 solid superbase. We employed various methods to characterize its structure and surface property, and examined its catalytic activity towards *one-pot* synthesis of polyfunctionalized 4*H*-pyrans through the condensation of aldehydes, malononitrile and an active methylene compound.

2 Experimental

2.1 Chemicals and Reagents

Most of the reagents and chemicals (analytic grade unless stated otherwise) were purchased from Kemiou Chemical Reagent Company and Tianjin Damao Chemical Reagent Co. Ltd. (Tianjin, China). They were dehydrated using 3 Å molecular sieves at RT. Ethyl cyanoacetate, acetylacetone and malononitrile were purchased from Aladdin Chemistry Co. Ltd. (Shanghai, China). Cyclohexane was dried by sodium under reflux. Aldehydes were purified by reduced pressure distillation (to remove acid) prior to use.

2.2 Catalysts Preparation

Magnesium-tin composite oxides (denoted hereinafter as MgO–SnO_2) were prepared as shown in Scheme 1. First tin tetrachloride ($SnCl_4$) was dissolved in water to prepare a solution of 0.5 M; then 0.1 M KOH was added to the aqueous $SnCl_4$ solution and white precipitate appeared in a pH range of 5–7. After being washed and filtered out, the white precipitate was transferred to a flask, and 0.5 M KOH solution was added to it to prepare "solution A" with

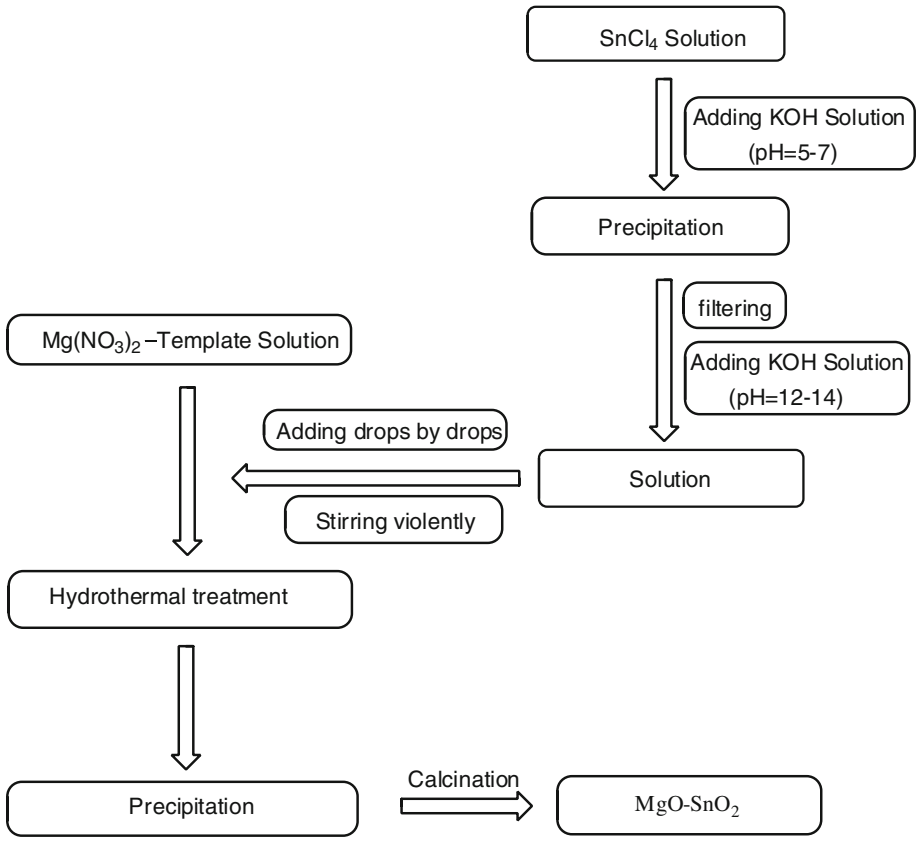

Scheme 1 Flow chart of MgO–SnO_2 preparation

pH of 12–14. Under vigorous stirring, "solution A" was added dropwise to 0.5 M aqueous solution of magnesium nitrate and P123 template. After the mixed solution was stirred at RT for 12 h, it was transferred to an autoclave and kept at 180 °C for 24 h. The crystallized precipitate was filtered out, washed and dried for 12 h to form a precursor. The MgO–SnO_2 was prepared by calcining the precursor at 550 °C for 2 h (5 °C/min for temperature rise) under high-purity N_2.

2.3 Characterization

X-ray diffraction (XRD) patterns were recorded on a Brucker D8 advance diffractometer with monochromatized Cu K_α radiation ($\lambda = 0.15406$ nm) at a setting of 40 kV and 40 mA. scanning electron microscopy (SEM) analyses were performed over a Hitachi S-4800 electron microscope operating at 2.0 kV. CO_2-TPD measurements for the estimation of surface basicity were conducted on a Micromeritics 2920 apparatus using thermal conductivity detector (TCD). The basicity of the as-prepared materials was also measured by the Hammett indicators method as described elsewhere [13, 31–33]. N_2 adsorption and desorption isotherms were measured using a Quantachrome Autosorb-1C/TCD Automatic Chemisorption & Physisorption Analyzer. The samples were degassed at 473 K under vacuum for 3 h prior to measurement. The Brunauer-Emmett-Teller specific surface area was calculated using adsorption data in the relative pressure range of 0.04–0.2. The total pore volume was determined from the amount of adsorbed N_2 at a relative pressure of about 0.95.

2.4 Catalyst Evaluation

Catalytic activity of the prepared materials was evaluated for the *one-pot* synthesis of polyfunctionalized 4*H*-pyrans through the condensation of aldehydes, malononitrile and an active methylene compound. The catalytic reactions were conducted in a 25 ml round-bottomed flask at RT using 1 mmol aldehyde, 1.1 mol malononitrile and 1.1 mmol acetoacetate derivatives without use of any solvent. The catalyst loading in all the cases was 0.035 g. After the reaction, the catalyst was separated from the mixture by centrifugation. The reaction mixtures were analyzed using an Agilent Technologies 7820 gas chromatograph equipped with FID and AB-FFAP capillary column (30 m × 0.25 mm × 0.25 μm). The conversion of benzaldehyde was determined using biphenyl as internal standard. All products were analyzed over an Agilent 6890-5973 MSD GC–MS equipment, and confirmed by ^{1}H NMR. The ^{1}H NMR spectra were recorded at 25 °C over an INOVA-400 M (Varian) instrument calibrated using tetramethyl silane as internal standard.

3 Results and Discussion

3.1 Catalyst Characterization

3.1.1 Hammett Indicators Method

We investigated the effect of Sn/Mg molar ratio on the basicity of MgO–SnO_2. As shown in Table 1, at Sn/Mg molar ratio of 4/1 and 2/1, the base strength of the as-synthesized materials is in the range of $15.0 \le H_- < 18.4$; while at Sn/Mg molar ratio of 1/2 and 1/4, the base strength is in the range of $22.5 \le H_- < 26.5$. The MgO–SnO_2 shows superbasicity only at Sn/Mg molar ratio of 1. The superbasic strength is $26.5 \le H_- < 33.0$, and the total superbasic sites is up to 0.833 mmol/g. Therefore, in this study, only MgO–SnO_2 with equimolar ratio of Sn/Mg was investigated.

3.1.2 CO_2-TPD

The CO_2-TPD result of MgO–SnO_2 (molar ratio of Mg/Sn = 1) is depicted in Fig. 1. In CO_2-TPD investigation, desorbed peaks at 423, 723 and 973 K indicate weak,

Table 1 Effect of Sn/Mg molar ratio on MgO–SnO_2 basicity

Sn/Mg molar ratio	Basic strength (H_-)	Superbasic sites (mmol/g)	Total basic sites (mmol/g)
4/1	$15.0 \le H_- < 18.4$	0	0.317
2/1	$15.0 \le H_- < 18.4$	0	0.761
1/1	$26.5 \le H_- < 33.0$	0.833	1.515
1/2	$22.5 \le H_- < 26.5$	0	1.308
1/4	$22.5 \le H_- < 26.5$	0	1.022

The basicity was measured by Hammett indicator method

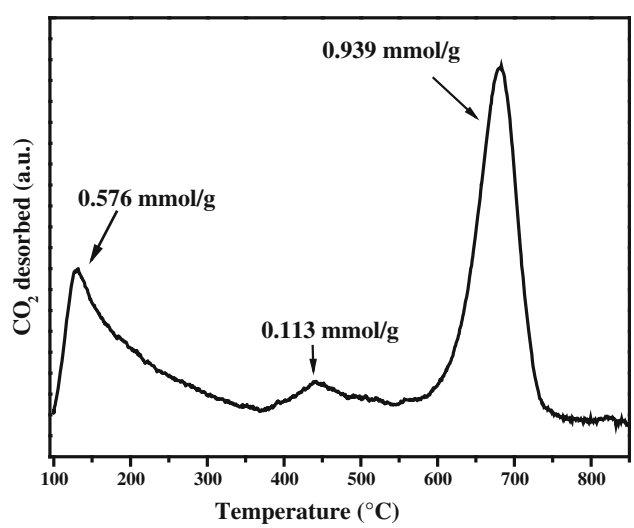

Fig. 1 CO_2-TPD profile of MgO–SnO_2

strong and superbasic sites, respectively [34, 35]. The amounts of these basic sites were calculated by the integral method based on the area of the corresponding desorption peaks; they are 0.576, 0.113 and 0.939 mmol/g, respectively. It is apparent that the distribution of base strength obtained from the results of Hammett indicators and CO_2-TPD methods are in good agreement with each other (Table 1; Fig. 1).

3.1.3 XRD

Figure 2 shows the XRD pattern of MgO–SnO_2. Compared to standard card of JCPDS 24-0723, it can be deduced that the weak diffraction peak is due to Mg_2SnO_4. There is no peak related to compounds such as MgO and SnO_2. It is plausible that both MgO and SnO_2 in the composite are amorphous. Since Mg^{2+} and Sn^{4+} are almost the same in diameter (Mg^{2+}: 0.66 Å, Sn^{4+}: 0.69 Å), it is easy for Mg^{2+} to intercalate into the defects of SnO_2 [36], hindering the crystallization of SnO_2 and enhancing the formation of superbasic sites.

3.1.4 N_2 Adsorption/Desorption Isotherm

As shown in Fig. 3, the N_2 adsorption/desorption isotherm of MgO–SnO_2 is typical of type-IV isotherm. According to the hystersis loop, MgO-SnO_2 is mesoporous in nature and possesses narrow pore diameter distribution [8], and the channels of such a dimension are favorable for the diffusion of reactants into the interior part of the catalyst. The specific surface area and pore volume of MgO–SnO_2 are 115.2 m^2/g and 0.348 ml/g, respectively. Generally, the specific surface area of MgO prepared by conventional method is not higher than 70 m^2/g [37]. Therefore, the

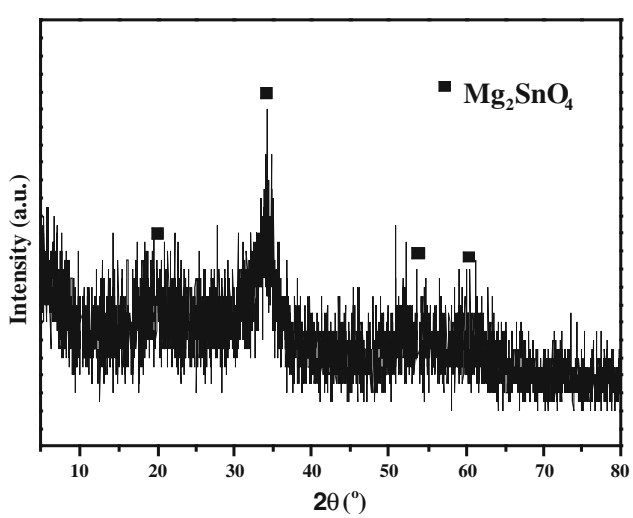

Fig. 2 XRD pattern of MgO–SnO_2

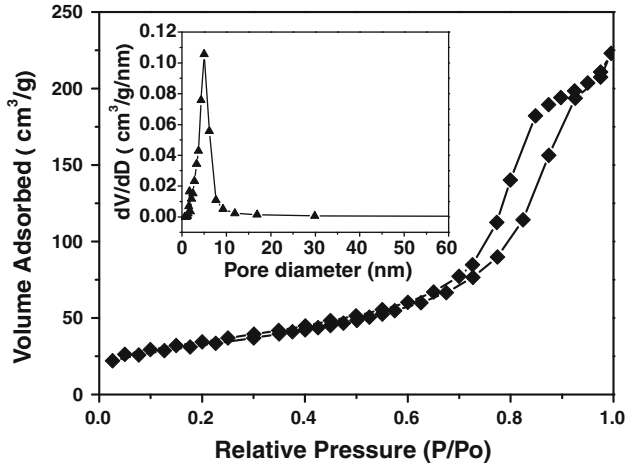

Fig. 3 N_2 adsorption/desorption isotherm and pore diameter distribution of MgO–SnO_2

introduction of SnO_2 into MgO not only improves superbasicty, but also increases the specific surface area.

3.1.5 SEM

Figure 4 shows the SEM images of MgO–SnO_2 prepared with and without the use of P123 template. It is obvious that the use of P123 template led to the formation of uniform spheres with diameter of ca. 150 nm. The SEM result is in accord with the N_2 adsorption/desorption isotherm. However, without the use of template, the MgO–SnO_2 is irregular in shape. Therefore, the presence of template shows important effect on the morphology of MgO–SnO_2.

3.2 Catalytic Performance

In order to evaluate the catalytic performance of MgO–SnO_2, one-pot synthesis of 4H-pyrans from benzaldehyde, malononitrile and ethyl acetoacetate was used as a model reaction, and MgO, SnO_2, CaO, KF/Al_2O_3 and MgO–Al_2O_3 were employed as reference catalysts. One can see from Table 2 that MgO–SnO_2 shows high catalytic activity towards this reaction, and the 4H-pyrans yield is up to 87.1 %, much higher than that of MgO (49.7 %), SnO_2 (12.5 %), CaO (50.6 %), KF/Al_2O_3 (57.2 %) and MgO–Al_2O_3 (53.8 %). It is noted that compared to the use of amino-functionalized ionic liquid [23], tetrabutylammonium bromide [25], tetra-methyl ammonium hydroxide [26], (BMIm)BF_4 [27], SiO_2 [28], piperidine [29], and Mg/La oxide [30], the use of the superbases results in much better catalytic efficiency; also the process is simpler and the reaction conditions milder. By correlation of the catalytic performance and the basicity of these catalysts in Table 2, one can deduce that strong basicity is beneficial for this reaction, which is similar to the results in the ref. [30].

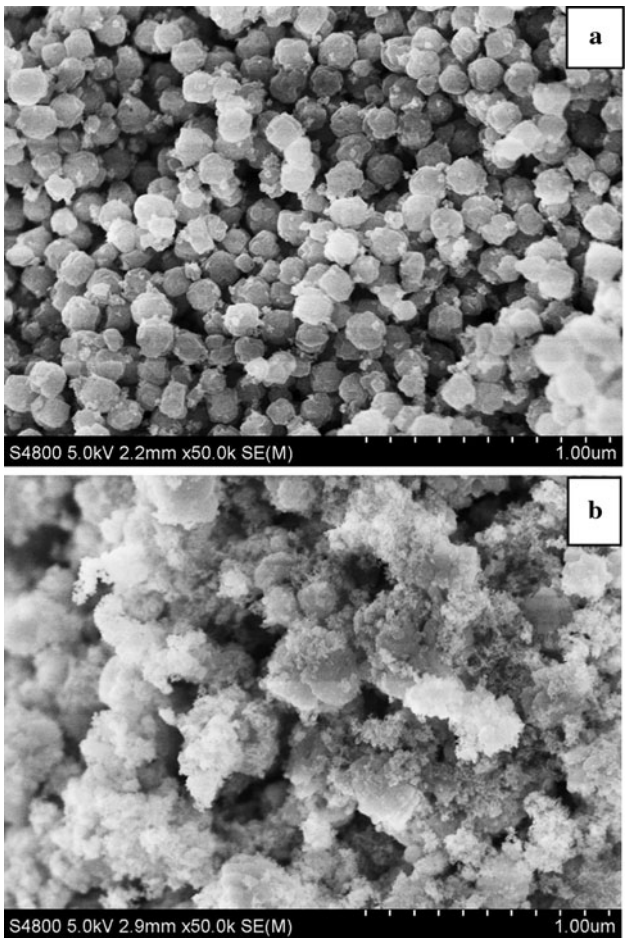

Fig. 4 SEM images of MgO–SnO_2 generated using **a** P123 as template, **b** no template

The MgO–SnO_2 was further investigated for one-pot synthesis of 4H-pyrans using various aldehydes as substrates (Table 3). One can see that in all cases products were generated in good to excellent yield. It is observed that the structures and properties of substrates have an effect on the 4H-pyrans synthesis. It is clear that the aldehydes with electron-withdrawing group (entries 2, 5, 9) are more reactive than those with electron-donating group (entries 3, 4, 8). For example, a conversion of 93.6 % is observed when chlorobenzaldehyde is used, while conversion is 59.3 % when 4-methylbenzaldehyde is used as substrate. The catalyst also shows good efficiency when aliphatic aldehyde is used as substrate (entry 6, yield: 90.6 %). It is noted that in all cases the product selectivity is 100 %. In addition, it is obvious that good yield is obtained when ethyl acetoacetate is changed to acetylacetone (entries 7–9).

To test the reusability of catalyst and reproducibility of catalytic performance, the superbasic MgO–SnO_2 catalyst was subject to cycles of reaction. Between cycles, separation of liquid product from catalyst was achieved by centrifugation, and the catalyst was directly reused for the next run. As shown in Table 3, the decline of benzaldehyde conversion and pyrans selectivity is minimal in a test of five cycles (entry 1), showing that the catalyst is stable and suitable for reuse.

3.3 Plausible Reaction Mechanism

Based on our results and those reported in literatures [26, 30, 38–40], we proposed a mechanism for the *one-pot* synthesis of polyfunctionalized 4*H*-pyrans from the condensation of aldehydes, malononitrile and an active methylene compound (Scheme 2). The surface O^{2-} ions of the solid superbase act as active basic sites to abstract H^+ from malononitrile, resulting in the generation of electron-rich dicyanomethylene anions. Then the anions attack benzaldehyde to form olefin intermediate **1** (not shown). That is

Table 2 Comparison of different catalysts for one-pot synthesis of 4H-pyrans

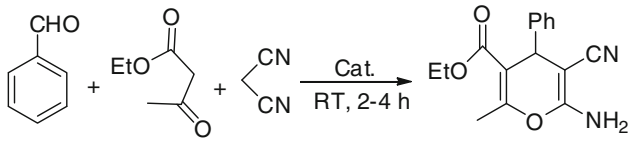

Entry	Catalyst[a]	Base strength (*H*_)	Time (h)	Yield (%)[b]
1	MgO	15.0–18.4	4	49.7
2	SnO_2	7.2–9.3	4	12.5
3	CaO	15.0–18.4	4	50.6
4	KF/Al_2O_3	18.4–22.5	4	57.2
5	MgO–Al_2O_3	18.4–22.5	4	53.8
6	MgO–SnO_2	26.5–33.0	2	87.1

Reaction conditions: benzaldehyde (1 mmol); malononitrile (1.1 mmol); ethyl acetoacetate (1.1 mmol); catalyst (0.035 g); RT

[a] Thermally treated at 550 °C for 2 h under high-purity N_2 atmosphere

[b] Products were purified by column separation method

Table 3 Superbasic MgO–SnO_2 as catalyst for the synthesis of various 4H-pyrans

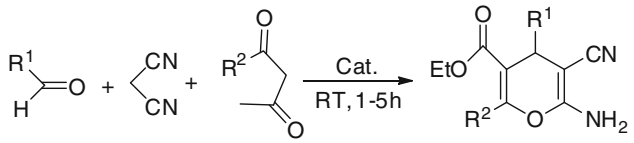

Entry	R^1	R^2	Time (h)	Yield[a] (%)
1	Ph	OEt	2	87.1, 85.5[b]
2	4-Cl-C_6H_4	OEt	3	93.6
3	4-Me-C_6H_4	OEt	3	72.8
4	4-OMe-C_6H_4	OEt	3	59.3
5	4-CF_3-C_6H_4	OEt	1	97.1
6	n-C_7H_{14}	OEt	1.5	90.6
7	Ph	Me	5	75.2
8	4-OMe-C_6H_4	Me	5	65.0
9	4-CF_3-C_6H_4	Me	5	93.4

Reaction conditions: aldehyde (1 mmol), malononitrile (1.1 mmol), ethyl acetoacetate or acetyl acetone (1.1 mmol)

[a] Isolated yield

[b] Isolated yield of the fifth recycle

to say, the Knoevenagel condensation reaction takes place between malononitrile and benzaldehyde to form intermediate **1**. The superbasic sites can also abstract H^+ from the acetylacetate derivates to form anions **2**, and the Michael addition reaction happens between intermediate **1** and anions **2**, forming acetylacetate derivates to yield intermediate **3**. Then with two steps of rearrangements in carbon framework, intermediates **4** and **5** are formed. Finally the abstracted H^+ attacks the NH^- of intermediate **5** to form the polyfunctionalized 4*H*-pyrans.

4 Conclusions

A novel mesoporous MgO–SnO_2 solid superbase in the form of spheres possessing high surface area of 115.2 m^2/g was synthesized. Its base strength is in the range of 26.5–33.0 with superbasic amount up to 0.939 mmol/g. The superbase exhibits excellent catalytic efficiency towards the *one-pot* synthesis of polyfunctionalized 4*H*-pyrans through the condensation of aldehydes, malononitrile and an active methylene compound, much higher than

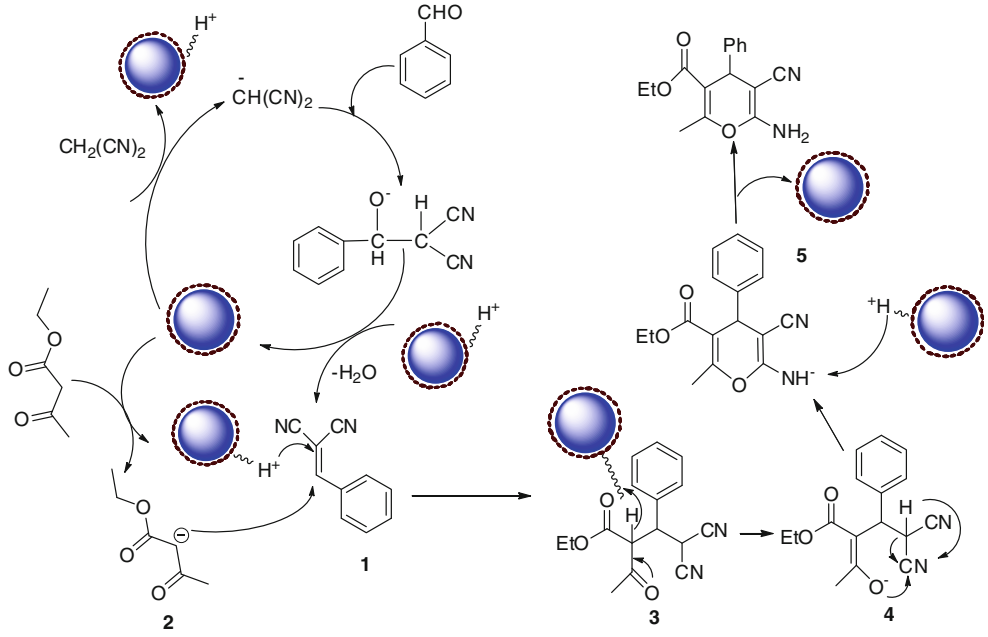

Scheme 2 Possible reaction mechanism for one-pot synthesis of polyfunctionalized 4H-pyrans over MgO–SnO_2

the catalysts reported in the literature. By simple thermal treatment of precursor under an atmosphere of high-purity nitrogen, composite oxide superbases can be generated. The results open up a new route for the design and synthesis of composite oxide superbase material. The use of the solid superbase is a suitable strategy for high-efficiency synthesis of polyfunctionalized 4*H*-pyrans, having advantages such as mild reaction temperature, low waste pollutants, good resuability and recyclability, excellent selectivity and yield, as well as short reaction time. It is envisaged that the route will find wide applications in the sectors of catalysis and fine chemical industry. Further investigation is under way: (i) to disclose the formation mechanism of superbasic sites, (ii) to confirm the nature of catalytically active sites, and (iii) to widen the catalytic applications of this class of superbase-type materials.

Acknowledgments This project was financially supported by the National Natural Science Foundation of China (Grant Nos. U1162109, 20873038), Hunan Provincial Natural Science Foundation of China (10JJ1003), the program for New Century Excellent Talents in Universities (NCET-10-0371), the Fundamental Research Funds for the Central Universities, and National 863 Program of China (2009AA05Z319). C.T. Au thanks the Hunan University for an adjunct professorship.

References

1. Tanabe K, Misono M, Ono Y, Hattori H (1989) New solid acids and bases. Their catalytic properties, University of Tokyo, Tokyo, p 3
2. Hattori H (1995) Chem Rev 95:537
3. Wei YD, Zhang SG, Li GX, Yin SY, Au CT (2011) Chin J Catal 32:891
4. Bota RM, Houthoofd K, Grobet PJ, Jacobs PA (2010) Catal Today 152:99
5. Gorzawski H, Hoelderich WF (1999) Appl Catal A: Gen 179:131
6. Sun N, Klabunde KJ (1999) J Catal 185:506
7. Li X, Lu GZ, Guo YL, Guo Y, Wang YQ, Zhang ZG, Liu XH, Wang YS (2007) Catal Commun 8:1969
8. Sun LB, Yang J, Kou JH, Gu FN, Chun Y, Wang Y, Zhu JH, Zou ZG (2008) Angew Chem Int Ed 47:3418
9. Wang Y, Huang WY, Chun Y, Xia JR, Zhu JH (2001) Chem Mater 13:670
10. Yin SF, Xu BQ, Wang SJ, Au CT (2006) Appl Catal A: Gen 301:202
11. Tsuji H, Kabashima H, Kita H, Hattori H (1995) React Kinet Catal Lett 56:363
12. Sun LB, Kou JH, Chun Y, Yang J, Gu FN, Wang Y, Zhu JH, Zou ZG (2008) Inorg Chem 47:4199
13. Zhang SG, Wei YD, Yin SF, Au CT (2011) Catal Commun 12:712
14. Zhang SG, Wei YD, Yin SF, Luo SL, Au CT (2011) Appl Catal A: Gen 406:113
15. Zhang SG, Wei YD, Yin SF, Chao C, Luo SL, Au CT (2011) Catal Commun 12:1333
16. Zhu JH, Wang Y, Chun Y, Wang XS (1998) J Chem Soc Faraday Trans 94:1163
17. Liu Z, Dong L, Ji W, Chen Y (1998) J Chem Soc Faraday Trans 94:1137
18. Godinho KG, Walsh A, Watson GW (2009) J Phys Chem C 113:439
19. Chen HT, Xiong SJ, Wu XL, Zhu J, Shen JC (2009) Nano Lett 9:1926
20. Gonzalez R, Martin N, Seoane C, Marco JL, Albert A, Cano FH (1992) Tetrahedron Lett 33:3809
21. Liu Y, Zhang J, Xu W (2007) Curr Med Chem 14:2872
22. Wang JL, Liu D, Zhang ZJ, Shan S, Han X, Srinivasula SM, Croce CM, Alnemri ES, Huang Z (2000) Proc Natl Acad Sci 97:7124
23. Peng Y, Song G (2007) Catal Commun 8:111
24. Fotouhi L, Heravi MM, Fatehi A, Bakhtiari K (2007) Tetrahedron Lett 48:5379
25. Jin TS, Xiao JC, Wang SJ, Li TS, Song XR (2003) Synlett: 2001
26. Balalaie S, Sheikh-Ahmadi M, Bararjanian M (2007) Catal Commun 8:1724
27. Rad-Moghadam K, Youseftabar-Miri L (2011) Tetrahedron Lett 67:5693
28. Banerjee S, Horn A, Khatri H, Sereda G (2011) Tetrahedron Lett 52:1878
29. Lu GP, Cai C (2011) J Heterocyclic Chem 48:124
30. Babu NS, Pasha N, Rao KT, Prasad PS, Lingaiah N (2008) Tetrahedron Lett 49:2730
31. Walling C (1950) J Am Chem Soc 72:1164
32. Benesi HA (1956) J Am Chem Soc 78:5490
33. Benesi HA (1957) J Phys Chem 61:970
34. Sun NJ, Klabunde KJ (1999) J Catal 185:506
35. Gorzawski H, Hoelderich WF (1999) J Mol Catal A: Chem 144:181
36. Corma A, Iborra S (2006) Adv Catal 49:239
37. Kabashima H, Shibuya HT, Hattori H (2000) J Mol Catal A: Chem 155:23
38. Fotouhi L, Heravi MM, Fatehi A, Bakhtiari K (2007) Tetrahedron Lett 48:5379
39. Bayat M, Shiraz NZ, Asayesh SS (2010) J Heterocyclic Chem 47:857
40. Ye ZJ, Xu RB, Shao XS, Xu XY, Li Z (2010) Tetrahedron Lett 51:4991